

Modification of mesoporous silica SBA-15 with different organic molecules to gain chemical sensors: a review

N. Lashgari^a, A. Badiei^{a,b,*} and G. Mohammadi Ziarani^c

^a*School of Chemistry, College of Science, University of Tehran, Tehran, Iran*

^b*Nanobiomedicine Center of Excellence, Nanoscience and Nanotechnology Research Center, University of Tehran, Tehran, Iran*

^c*Department of Chemistry, Faculty of Science, Alzahra University, Tehran, Iran*

(Received 21 October 2015, Accepted 2 November 2015)

ABSTRACT: The recognition of the biologically and environmentally important ions is of great interest in the field of chemical sensors in recent years. The fluorescent sensors as a powerful optical analytical technique for the detection of low level of various analytes such as anions and metal cations have been progressively developed due to the simplicity, cost effective, and selectivity for monitoring specific analytes in various systems. Organic-inorganic hybrid nanomaterials have important advantages as solid chemosensors and various innovative hybrid materials modified by fluorescence molecules were recently prepared. On the other hand, the homogeneous porosity and large surface area of mesoporous silica make it a promising inorganic support. SBA-15 as a two-dimensional hexagonal mesoporous silica material with stable structure, thick walls, tunable pore size, and high specific surface area is a valuable substrate for modification with different organic chelating groups. This review highlights the fluorescent chemosensors for ionic species based on modification of the mesoporous silica SBA-15 with different organic molecules, which have been recently developed from our laboratory.

Keywords: *SBA-15; Surface modification; Hybrid materials; Fluorescent chemosensors*

INTRODUCTION

The molecular design and construction of chemosensors to detect biologically and environmentally important ionic species are currently of great interest [1,2]. Several analytical techniques, such as mass spectrometry, high performance liquid chromatography, ion sensitive electrodes, and atomic absorption spectroscopy have been used to monitor the concerned targets. However, their wide utilization is largely limited due to their extremely high cost and time consuming procedures together with the use of sophisticated instrumentation. In this regard, the techniques based on fluorescence sensors present a number of appealing advantages in terms of high selectivity, high sensitivity and instantaneous response to these species [3-5].

Very recently, covalent immobilization of organic chelating groups onto the inorganic nanomaterial substrates

has attracted extensive interest in the field of fluorescent sensor [6]. These hybrid materials have important advantages. First, immobilized receptors on inorganic supports can liberate the guest molecules (metal ions or anions) from the pollutant solution. Second, the solid chemosensors display extremely high selectivity and sensitivity to the fluorescence and absorption changes compared to spherical structures because of their larger surface areas and well-defined pores. Finally, the organic-inorganic hybrid nanomaterials can be recycled by suitable chemical treatment.

Among various nanomaterials, mesoporous silica materials are promising inorganic supports due to having many advantages such as tunable pore size, stable structure, and high specific surface area with abundant Si-OH active bonds on the pore walls or surface [7]. Therefore, silica nanomaterials were the first choice for the preparation of functionalized nanosensors [8-14].

SBA-15, a hexagonally ordered mesoporous silica, first

*Corresponding author. E-mail: abadiei@khayam.ut.ac.ir

prepared by Zhao *et al.* [15], appears to be more attractive as the sensor scaffold. In addition to their use as chemosensors, functionalized SBA-15 materials have been increasingly used as catalysts [16], adsorbents [17,18] and carrier materials in drug delivery [19-21]. Though SBA-15 itself is non-fluorescent, it is suitable as a sensor scaffold because it can supply a high surface area covered with a layer of hydroxyl groups that can act as binding sites for covalent grafting of silanes on a silicon wall. Particularly, the reason that SBA-15 can supersede other mesoporous materials is that its ordered structure can maintain after occlusion of guest molecules, deriving from the thicker wall that aids to the maintenance of the structural integrity [22]. There are two main methods to modify the surface of SBA-

15: direct synthesis or post-grafting [23,24]. In this current review, we focus on the fluorescent chemosensors for metal ions and anions based on modification of mesoporous silica SBA-15 with different organic molecules, which have been recently developed from our laboratory.

MODIFICATION OF SBA-15 WITH ORGANIC MOLECULES AND ITS ROLE AS A CHEMOSENSOR

One of the interesting molecules for incorporation into the channels of mesoporous silicas is 8-hydroxyquinoline (HQ) and its derivatives due to their chelating ability towards various metal ions and high luminescence

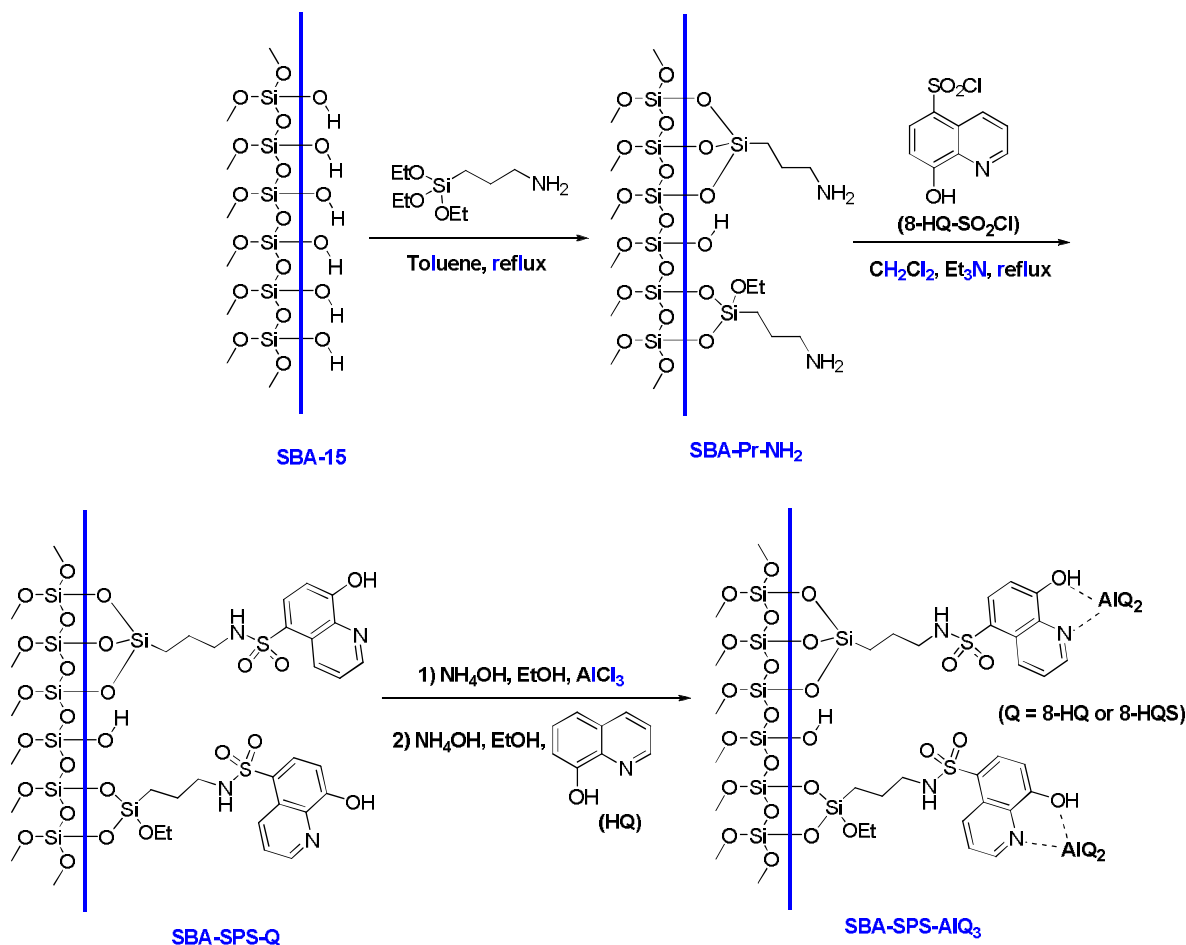


Fig. 1. Synthesis route of SBA-SPS-AIQ₃.

efficiency of resulting metal complexes [25-27]. In 2011, our group presented a new method for covalently linking 8-HQ in nanochannels of SBA-15 in two steps: attachment of aminopropyl on SBA-15 followed by covalent linkage of 8-HQ *via* stable sulfonamide bond and then aluminum complexes of 8-HQ was covalently bonded to SBA-SPS-Q (Fig. 1) [28]. The prepared materials were characterized by powder X-ray diffraction (XRD), scanning electron microscopy (SEM), transmission electron microscopy (TEM), fourier transform infrared (FT-IR), N₂ adsorption/desorption, and thermal analysis (TGA-DTA). Figure 2 shows the low angle XRD patterns of SBA-15 and the functionalized SBA-15 with amine and 8-HQ groups. All samples have a single intensive reflection at 2 θ angle around 0.85° similar to the typical SBA-15 materials. However, in the case of functionalized SBA-15 materials the peak (100) intensity decreases after immobilizations due to the difference in the scattering contrast of the pores and the walls, and to the erratic coating of organic groups on the nano-channels. Figure 3 illustrates the SEM and TEM images of SBA-SPS-Q. The SEM image (Fig. 3a) shows uniform particles about 1 μ m and the same morphology was observed for SBA-15. On the other hand, the TEM image (Fig. 3b) reveals the parallel channels, resembling the pore configuration of SBA-15. This indicates that the pore of SBA-SPS-Q has not collapsed during two steps of reaction and this is quite in agreement with the XRD results.

It was followed by the investigation of the interaction of aluminum ion with this fluorophore material using fluorescence spectroscopy. Figure 4 shows the photoluminescence (PL) spectra of all samples containing HQ. In the emission spectra of SBA-SPS-Q (Fig. 4a), intense luminescence was remarkably observed around 477 nm, while SBA-SPS-QAl and SBA-SPS-AlQ₃ exhibit a very intense fluorescence around 505 nm in the mixed solution (Fig. 4b and c). The observed blue shift in the fluorescence spectra of SBA-SPS-Al(QS)₃ (Fig. 4e) indicates that emission spectra of grafted complexes on the SBA-SPS-Q can be easily tuned through the ligand exchange reaction. In a related study, we also reported one pot synthesis of functionalized SBA-15 through co-condensation of tetraethylorthosilicate with an 8-hydroxyquinoline-5-sulfonamide-modified organosilane precursor in the presence of P123 as structure-directing

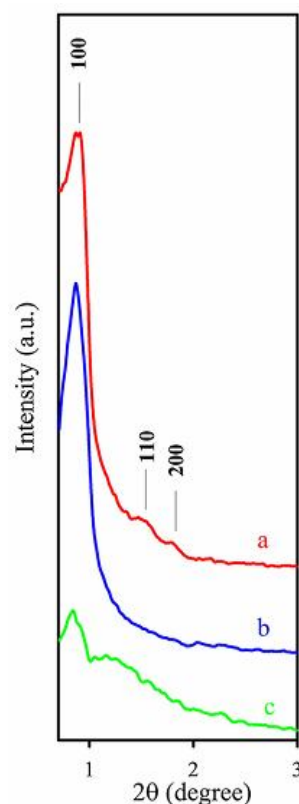


Fig. 2. XRD patterns for (a) SBA-15, (b) SBA-Pr-NH₂ and (c) SBA-SPS-Q [28].

agent [29]. Then, aluminum quinolate complex was attached covalently to this functionalized SBA-15 by using coordinating ability of grafted 8-HQ. Its emission spectra showed the characteristic fluorescence of the corresponding AlQ₃ complex in solution with a slightly blue shift in emission maximum.

Later on, it was found that SBA-SPS-AlQ_x has a high selectivity and sensitivity to detect Cr₂O₇²⁻ ion over other anions (Fig. 5). Therefore, this fluorescent nano-material may be used as a chemo-sensor for determination of dichromate anions in aqueous solutions [30]. By monitoring the fluorescence of SBA-SPS-AlQ_x with Cr₂O₇²⁻, a linear response is observed in the range of 0.16-2.9 μ M with the detection limit of 0.2 ng ml⁻¹.

In a similar study, SBA-SPS-AlQ_x showed a remarkable fluorescent quenching in the presence of MnO₄⁻ anion over other anions, because of the higher stability of its inorganic complex with permanganate anion (Fig. 6) [31]. In other

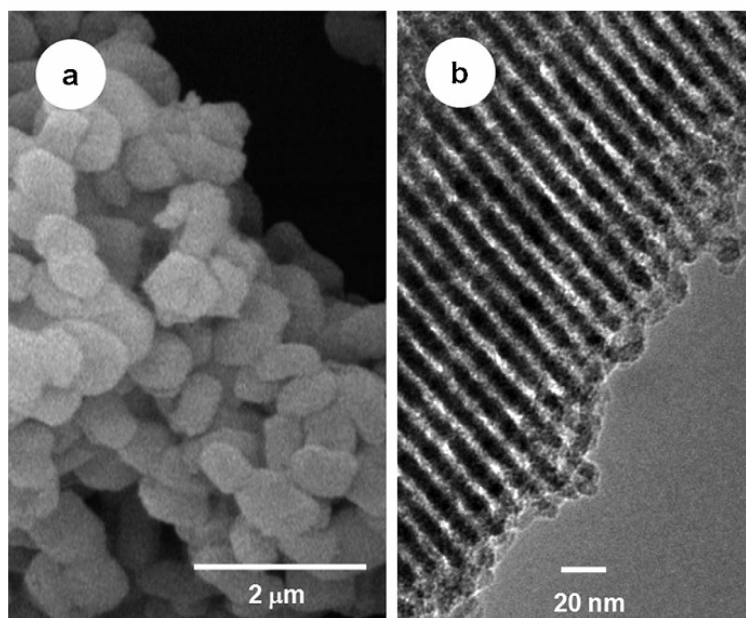


Fig. 3. SEM (a) and TEM (b) images of the SBA-SPS-Q compound [28].

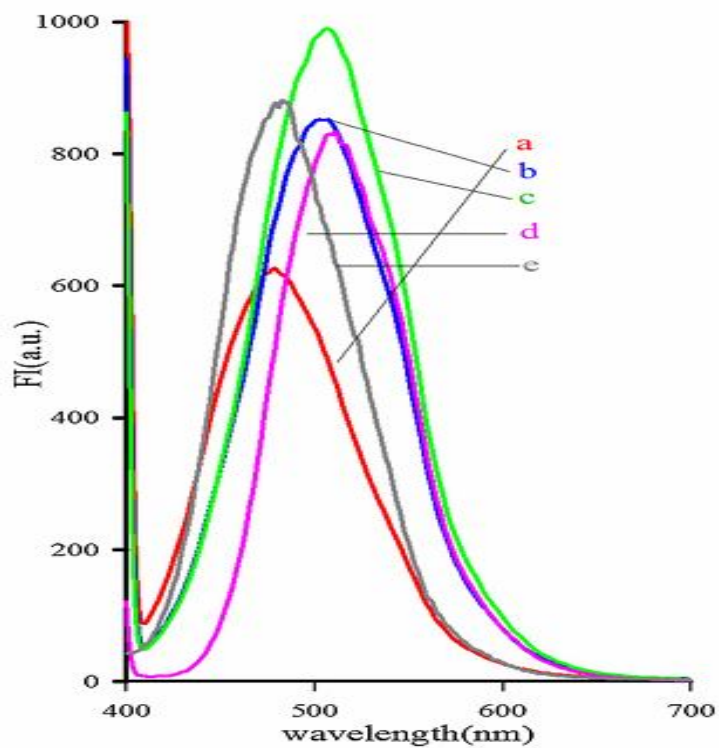


Fig. 4. Emission spectra excited at 377 nm of (a) SBA-SPS-Q, (b) SBA-SPS-QAl, (c) SBA-SPS-AlQ₃, (d) AlQ₃, and (e) SBA-SPS-Al(QS)₃ [28].

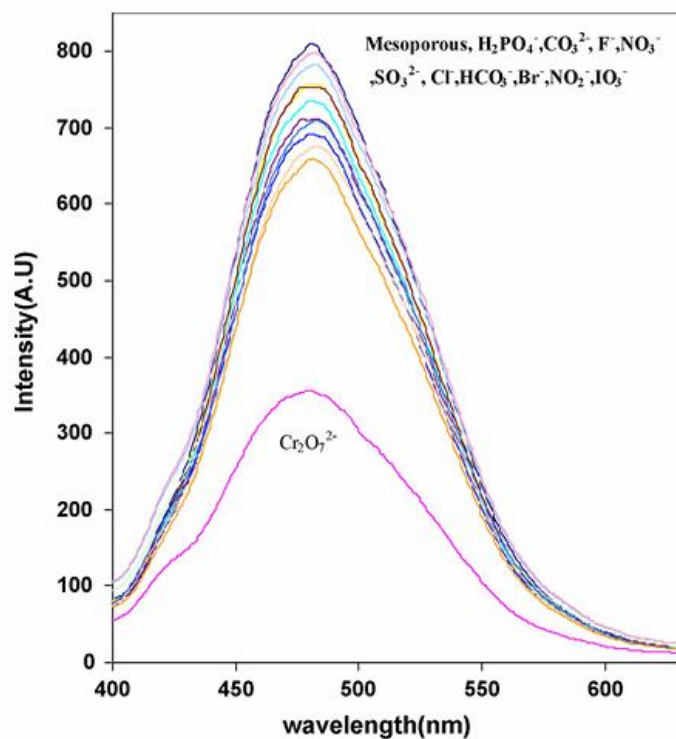


Fig. 5. Fluorescence response of SBA-SPS-AIQ_x upon addition of different anions in aqueous solution [30].

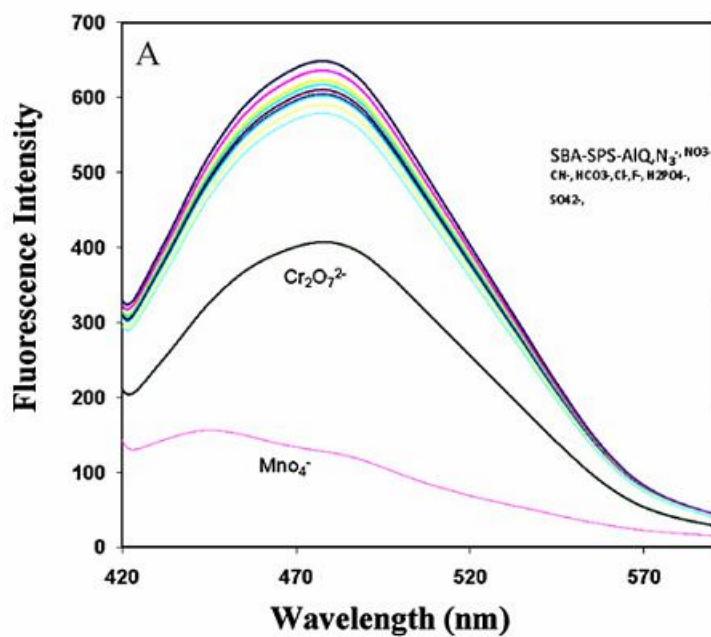


Fig. 6. Fluorescence emission spectra of SBA-SPS-AIQ_x in the presence of various anions [31].

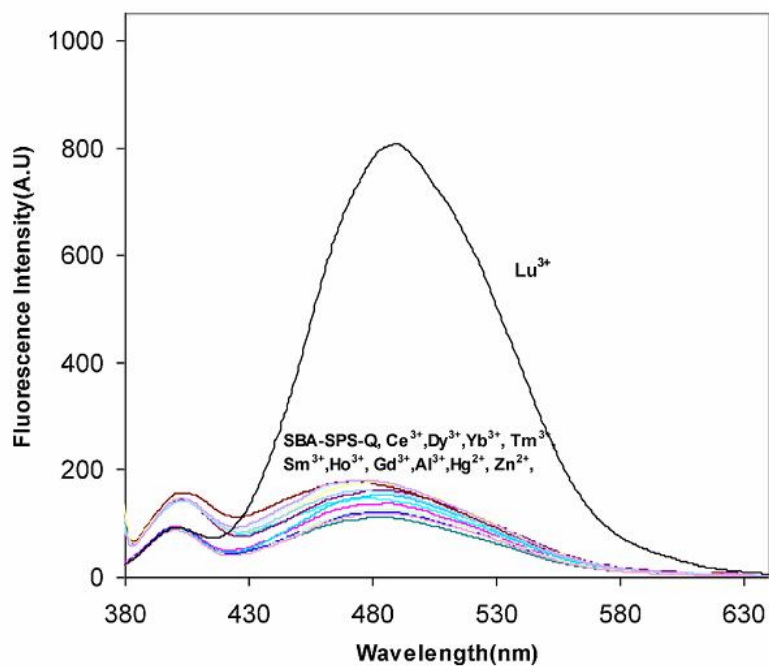


Fig. 7. Fluorescence emission spectra of SBA-SPS-Q suspended in an aqueous solution in the presence of different metal ions [34].

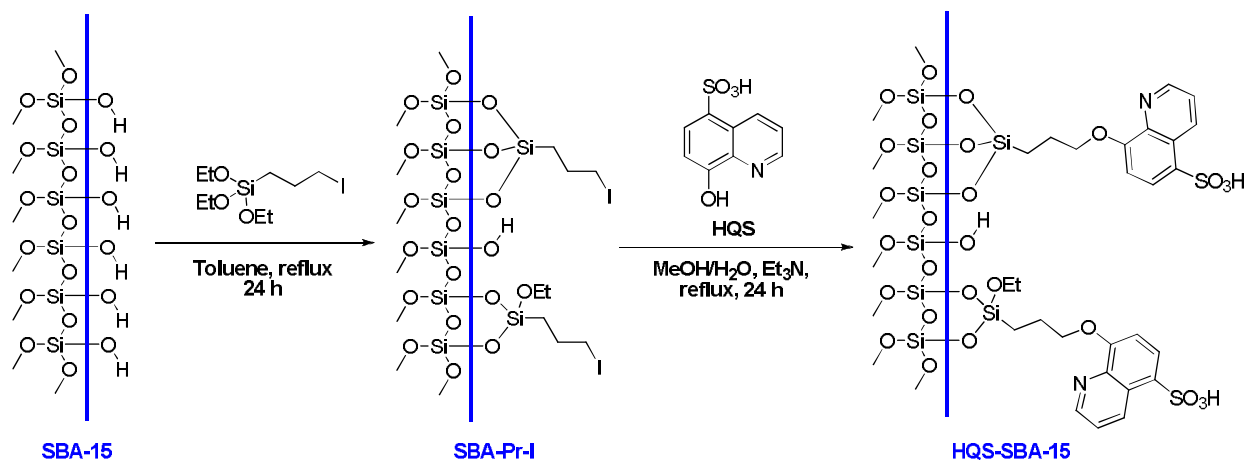


Fig. 8. The overall synthesis procedure of 8-hydroxyquinoline-5-sulfonic acid functionalized ordered nanoporous of SBA-15 (HQS-SBA-15).

related studies, modified SBA-15 was used as a selective sensing element in construction of a nano-composite carbon paste electrode for measurement of permanganate [32] and dichromate ions [33].

Studies on fluorescence properties of SBA-SPS-Q reveal a selective interaction between SBA-SPS-Q and Lu^{3+} ion (Fig. 7) [34]. The enhancement of fluorescence is attributed to the strong covalent binding of Lu^{3+} ion, evident from the large binding constant value. This chemosensor has been applied to determine Lu^{3+} ion in some soil samples where domestic devices were stored.

A novel modified SBA-15 with 8-hydroxyquinoline-5-sulfonic acid (HQS-SBA-15) as a hybrid optical sensor was prepared by a two-step post synthesis of SBA-15: functionalization with 3-(iodopropyl)-trimethoxysilane followed by the covalent attachment of 8-hydroxyquinoline-5-sulfonic acid (Fig. 8) [35]. Based on fluorescence investigation of HQS-SBA-15, colloidal suspensions of this matter in water make possible detecting selectively and sensitively two ions with opposite charges, *i.e.* Pb^{2+} and I^- ions, in the presence of interfering cations and different interfering anions, respectively (Figs. 9 and 10). It was

verified that HQS-SBA-15 sensor functions reversibly and is applicable in a wide range of pH values and is able to determine the presence of the ions in real samples. Moreover, good linearity was obtained between the fluorescence emission of HQS-SBA-15 and $[\text{Pb}^{2+}]$ and $[\text{I}^-]$ with detection limits of 1.7×10^{-6} and 2.1×10^{-6} for Pb^{2+} and I^- , respectively.

In a study toward functionalization of SBA-15 materials with fluorene, grafting of fluorene onto the pores of SBA-15 was performed *via* attachment of three different organosilica with one, two, and three amine groups followed by covalent linkage of fluorene (Fig. 11) [36]. The sensing ability of aqueous suspended solution of FM-SBA-15, FD-SBA-15 and FT-SBA-15 was studied by addition of the cations Fe^{3+} , Cr^{3+} , Mg^{2+} , Co^{2+} , Ni^{2+} , Cu^{2+} , Hg^{2+} and Zn^{2+} . As shown in Fig. 12, of all the cations tested, addition of Fe^{3+} ion to a suspension of these materials resulted in the largest decrease in the fluorescence intensity. A good linearity between the fluorescence intensity of FM-SBA-15, FD-SBA-15 and FT-SBA-15 and the concentration of Fe^{3+} ion was constructed, which enabled these materials as fluorescence chemosensors for detecting the Fe^{3+} ion.

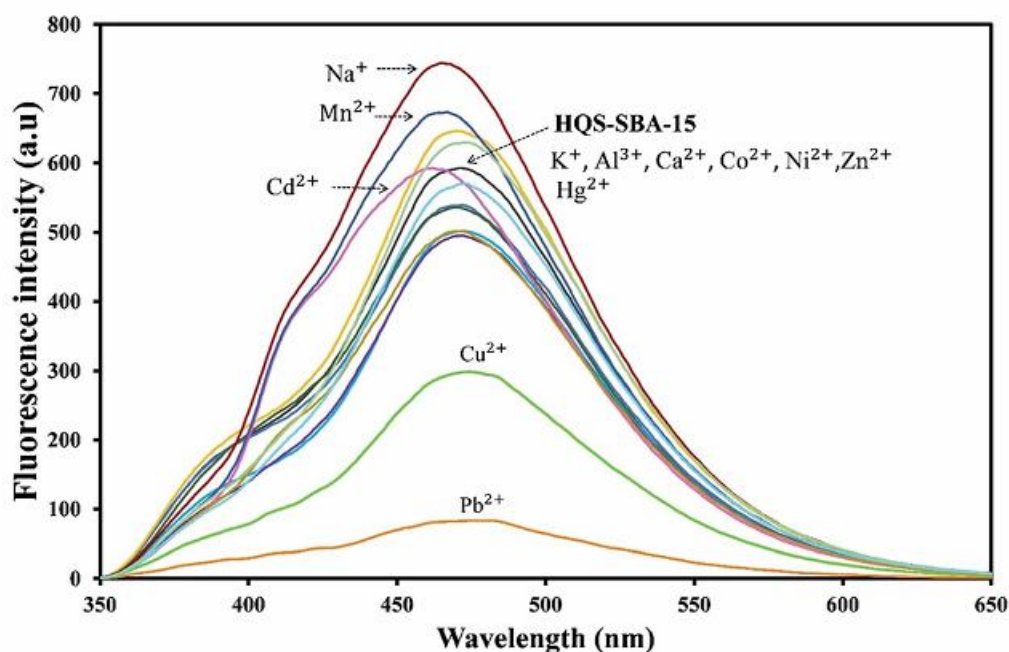


Fig. 9. Fluorescence spectra of the aqueous suspended HQS-SBA-15 in the presence of different metal cations [35].

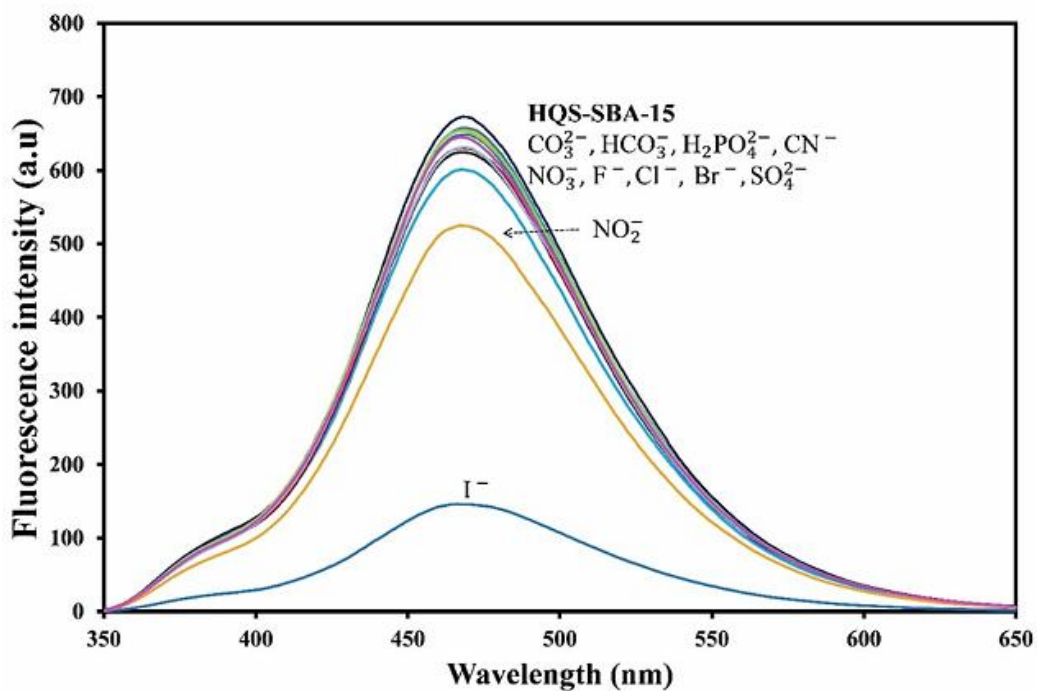


Fig. 10. Fluorescence spectra of the aqueous suspended HQS-SBA-15 in the presence of different anions [35].

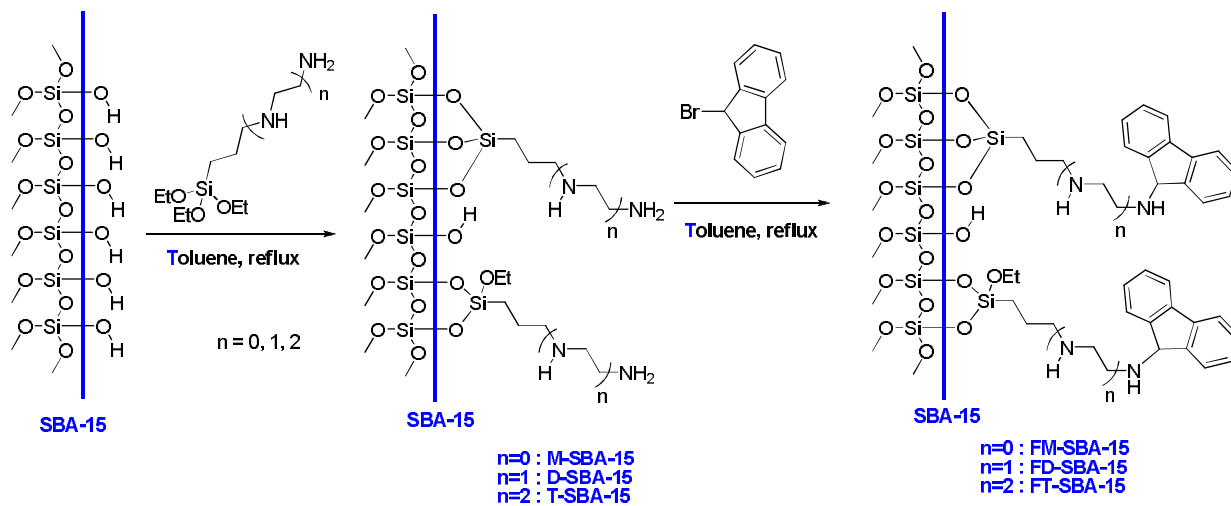


Fig. 11. Preparation of the functionalized mesoporous silica FM-SBA-15, FD-SBA-15 and FT-SBA-15.

Furthermore, the fluorescence spectrum of FM-SBA-15 in acidic media was studied (Fig. 13), and it showed one fluorescence emission at 305 nm in maximum absorption wavelength (260 nm) as a result of the interaction of H^+ with this material [37]. It was concluded that the structural change between FM-SBA-15 and the protonated form might be an effective candidate for acid-dependent molecular-sensor models for advanced application in molecular sensors in the future.

Motivated by the good results obtained from fluorene functionalized SBA-15, our group also tried to synthesize a new hybrid mesoporous chemosensor by utilizing a new derivative of fluorene *i.e.* bis(2-aminoethyl)-2-(9-fluorenyl)malonamide (FLen) (Fig. 14) [38]. The sensing ability of the obtained material was studied by addition of the cations Fe^{3+} , Cr^{3+} , Mg^{2+} , Co^{2+} , Ni^{2+} , Cu^{2+} , Hg^{2+} and Zn^{2+} to aqueous suspended solution of SBA-F. Among all metal ions, the sensor showed highly selective and sensitive

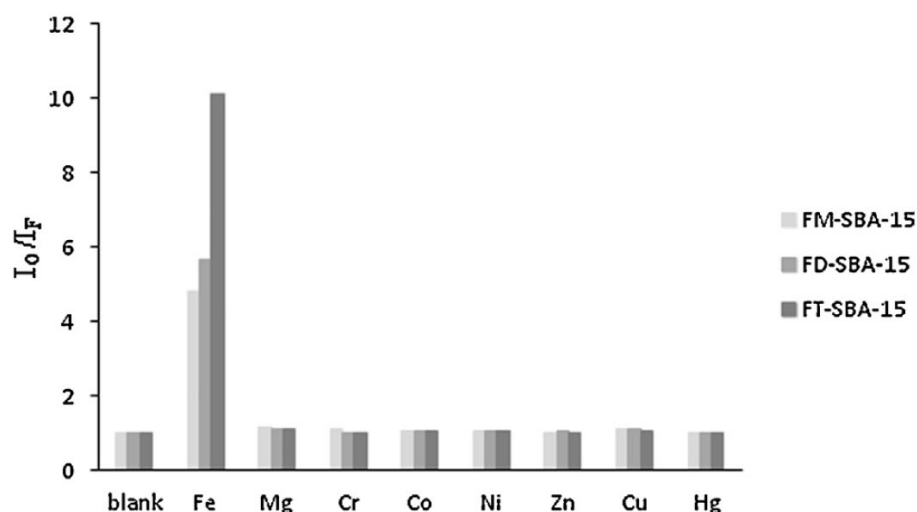


Fig. 12. Bar graphs of the fluorescence emission intensity for 8 different metal ions showing the metal ions selectivity profile of FM-SBA-15, FD-SBA-15 and FT-SBA-15 for each metal ion. I_0 corresponds to emission of FM-SBA-15, FD-SBA-15 and FT-SBA-15 without metal ions [36].

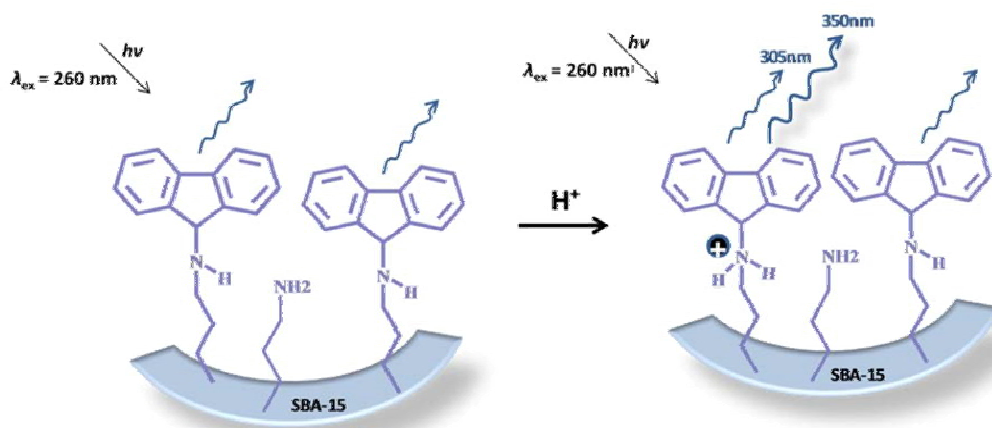


Fig. 13. Fluorescence emission of FM-SBA-15 and protonation of amine group [37].

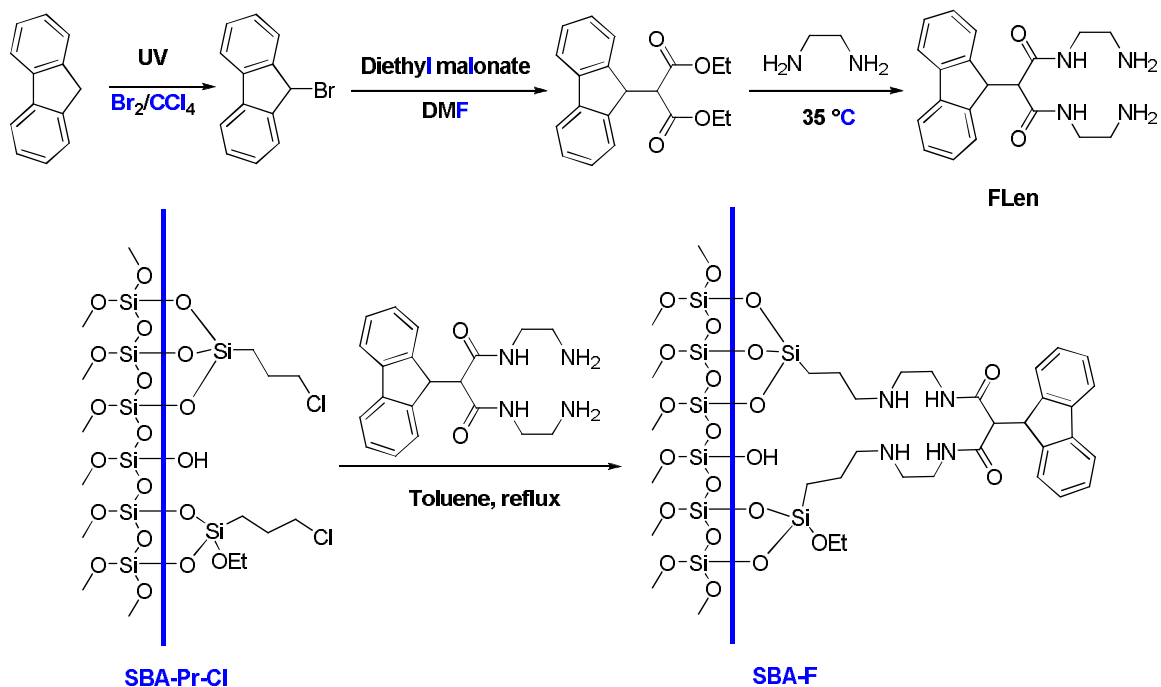


Fig. 14. Modification of SBA-15 with the synthesized bis(2-aminoethyl)-2-(9-fluorenyl)malonamide.

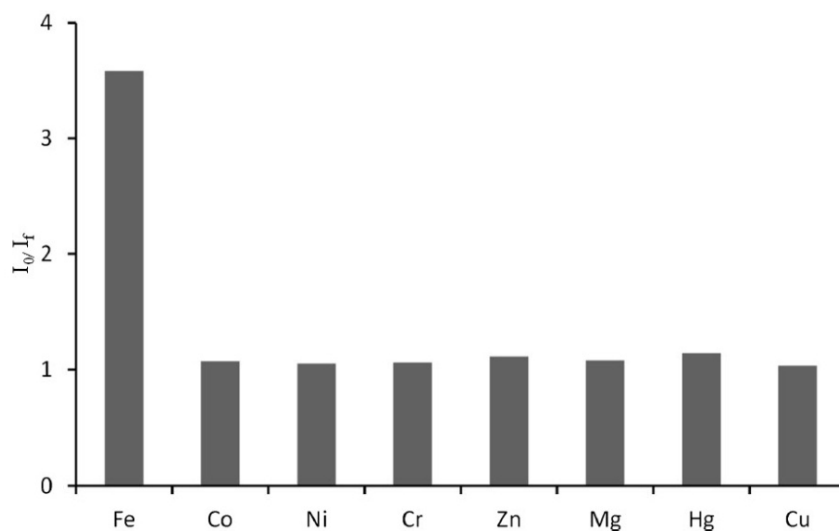


Fig. 15. Bar graphs of the fluorescence emission intensity of SBA-F for Fe^{3+} , Cr^{3+} , Mg^{2+} , Co^{2+} , Ni^{2+} , Cu^{2+} , Hg^{2+} and Zn^{2+} cations. I_0 corresponds to emission of SBA-F in the absence of metal ions [38].

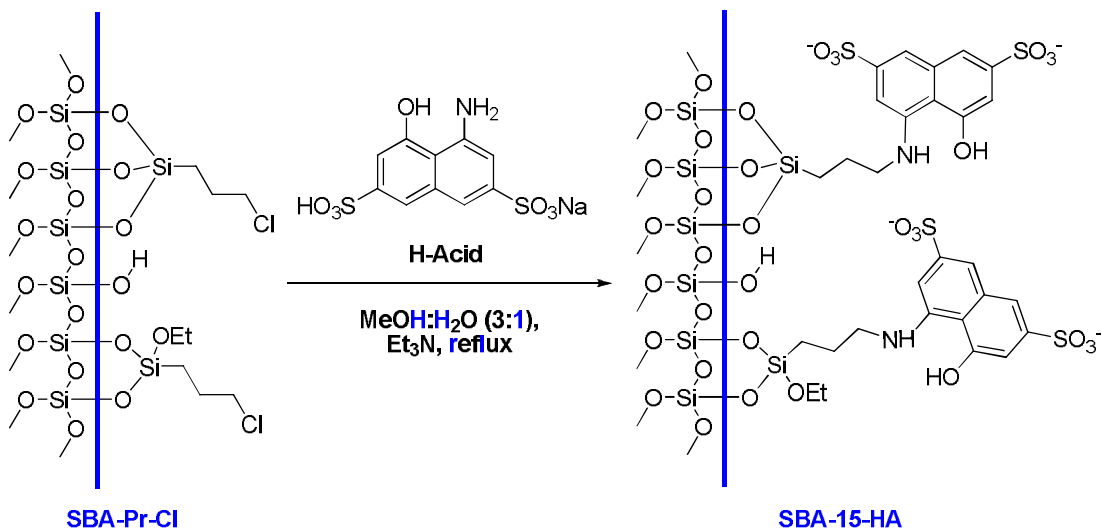


Fig. 16. Schematic representation of SBA-15-HA synthesis procedure.

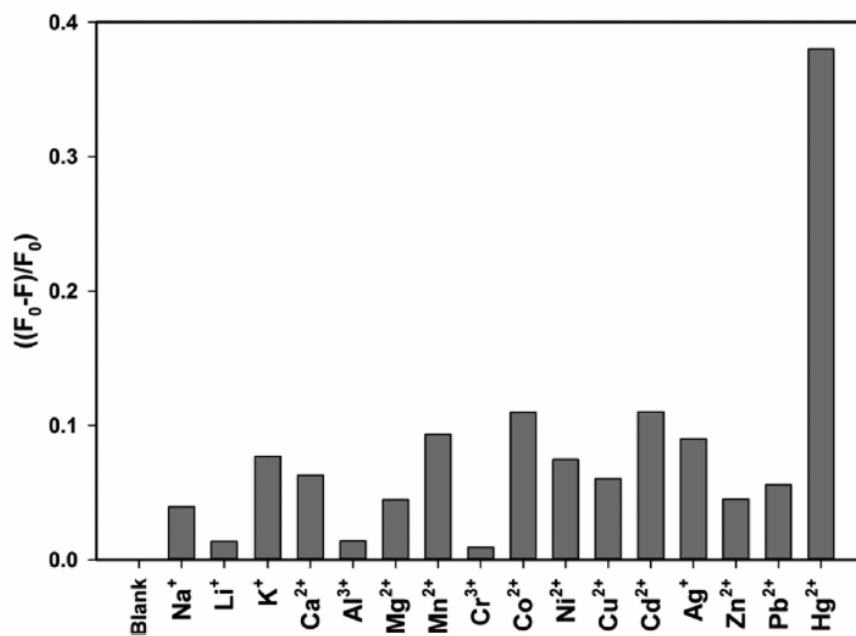


Fig. 17. The quenching ratio $((F_0 - F)/F_0)$ of fluorescence response of SBA-15-HA aqueous dispersion in the presence of various metal ions at pH 7.0 [39].

recognition toward Fe^{3+} . When Fe^{3+} was added to the solution, a significant decrease of the fluorescence intensity was observed (Fig. 15). A good linearity between the fluorescence intensity of SBA-F and the concentration of Fe^{3+} ion was constructed with a suitable detection limit of 1.35×10^{-5} .

In a careful study, a fluorescent sensor was designed based on the attachment of 1-amino-8-naphthol-3,6-disulphonic acid (H-acid) to the SBA-15 mesoporous silica surface (SBA-15-HA) in a two-step modification process

(Fig. 16) [39]. The fluorescent sensing properties of SBA-15-HA were examined toward several metal ions including Li^+ , Na^+ , K^+ , Ag^+ , Ca^{2+} , Mg^{2+} , Al^{3+} , Mn^{2+} , Cr^{3+} , Cd^{2+} , Zn^{2+} , Pb^{2+} , Co^{2+} , Ni^{2+} , Cu^{2+} , and Hg^{2+} and the results showed high selectivity for Hg^{2+} (Fig. 17). Computational studies were accomplished to find a detailed electronic description for the quenching mechanism of H-acid fluorescence by Hg^{2+} ion as well as studying the structure and bonding in the [H-acid] Hg^{2+} complex (Fig. 18). Based on the computational results, a logical/rational mechanism for fluorescence

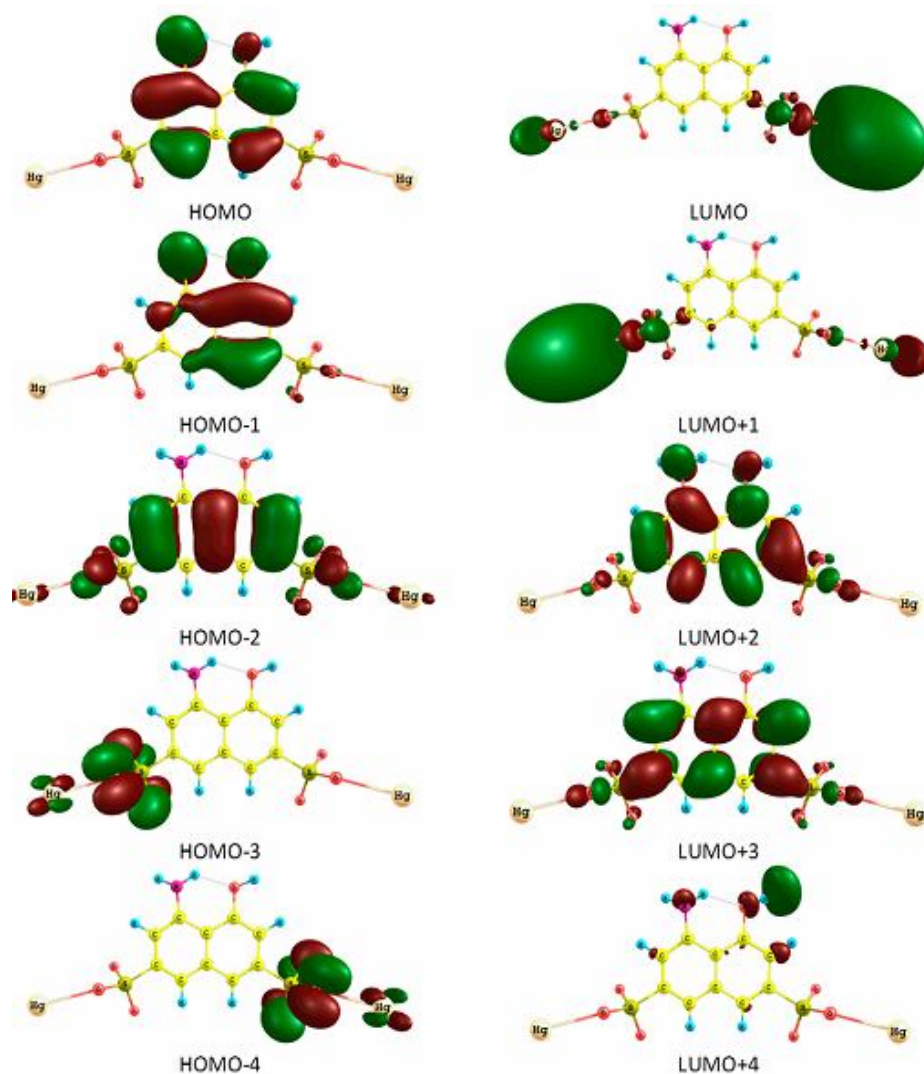


Fig. 18. Frontier molecular orbitals of [H-acid] Hg^{2+} calculated in aqueous solution at PBE0/6-31++G ** PCM level of theory [39].

quenching was proposed showing that the interaction between H-acid and Hg^{2+} ions alters the electronic structure of H-acid and converts its emissive lowest-lying excited state to a dark state which has been observed as fluorescence quenching.

In another publication from our group, a novel organic-inorganic hybrid optical sensor (SBA-NCO) was designed

and synthesized through immobilization of isocyanatopropyl-triethoxysilane and 1-amino-naphthalene on to the surface of SBA-15 by post-grafting method (Fig. 19) [40]. Fluorescence experiments demonstrated that SBA-NCO is a highly selective optical sensor for the detection of Fe^{3+} directly in water over a wide range of metal cations including Na^+ , K^+ , Mg^{2+} , Ca^{2+} , Cu^{2+} , Zn^{2+} , Mn^{2+} , Fe^{2+} , Co^{2+} ,

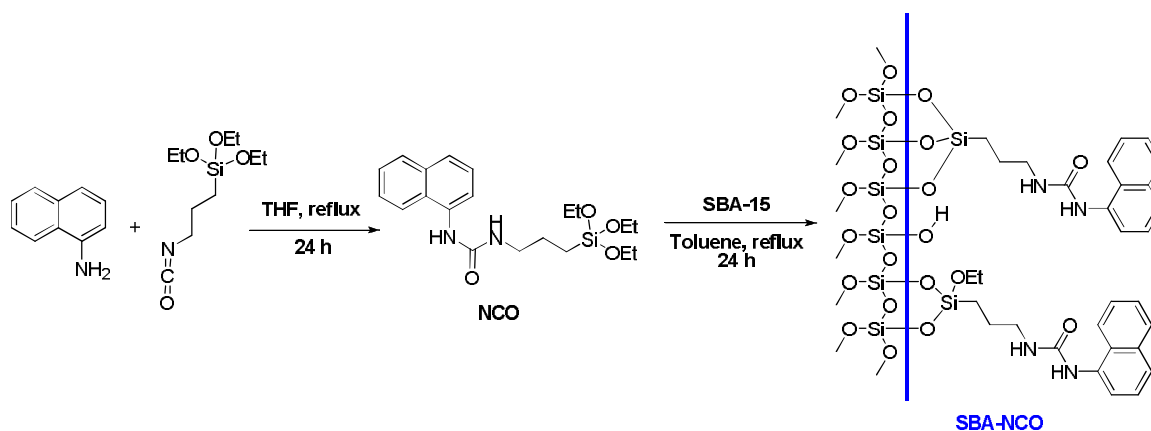


Fig. 19. Synthesis procedure of SBA-NCO.

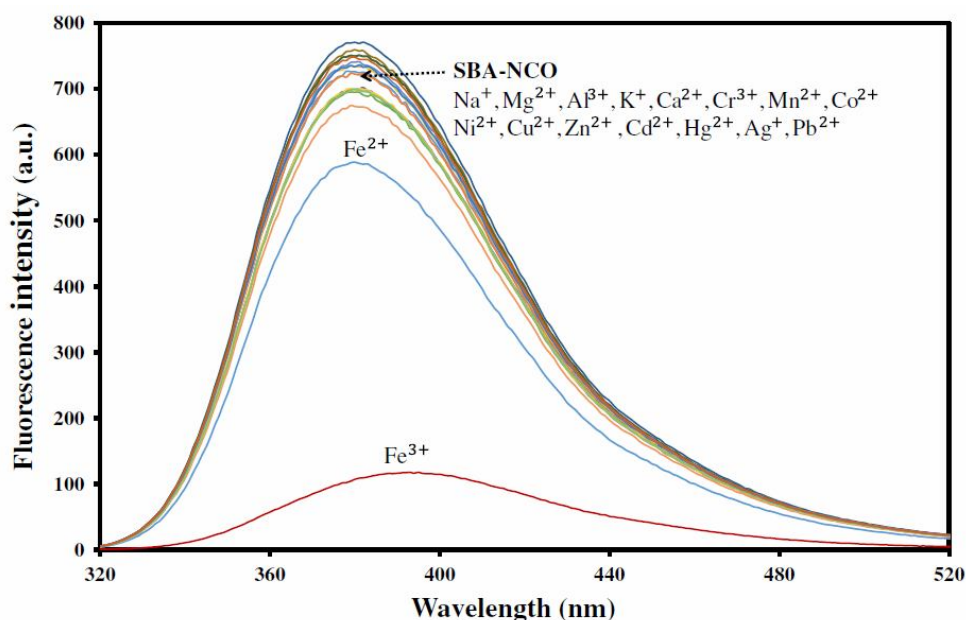


Fig. 20. Fluorescence spectra of the suspended SBA-15-NCO in the presence of various cations [40].

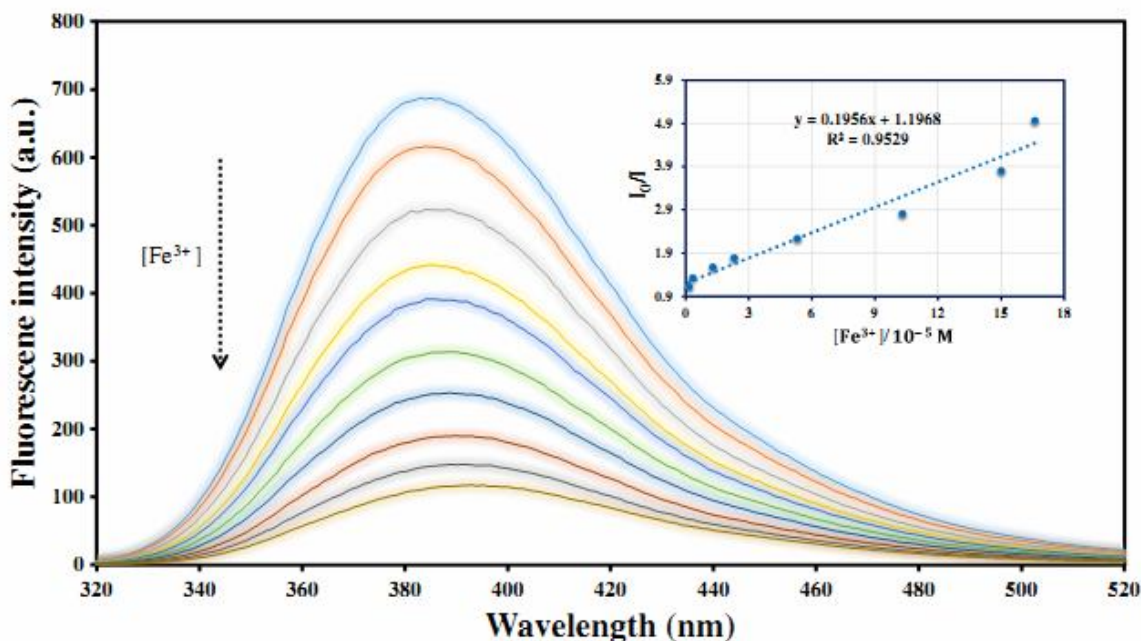


Fig. 21. The fluorescence response of the suspended SBA-15-NCO with different concentrations of Fe^{3+} . The inset is the Stern-Volmer plot [40].

Cd^{2+} , Pb^{2+} , Ni^{2+} , Cd^{3+} , Cr^{3+} , Al^{3+} , and Hg^{2+} in a wide pH values (Fig. 20). Moreover, a good linearity between normalized fluorescence intensity and concentration of Fe^{3+} ($r^2 = 0.9529$) with detection limit of 4.5×10^{-6} M was established (Fig. 21).

CONCLUSIONS

SBA-15 with a two-dimensional hexagonal structure which provides a high surface area, uniform open pores, thick walls, and high hydrothermal and thermal stability is a valuable substrate for modification with different organic chelating groups by the grafting method. This paper reviewed modification of SBA-15 with different organic molecules which have been recently developed from our laboratory to provide selective, sensitive, low cost, and rapid response optical sensors.

ACKNOWLEDGEMENTS

The authors thank the research council of University of

Tehran for financial support.

REFERENCES

- [1] B. Valeur, I. Leray, *Coord. Chem. Rev.* 205 (2000) 3.
- [2] M.A. Martín, A.I. Olives, B. del Castillo, J.C. Menéndez, *Curr. Pharm. Anal.* 4 (2008) 106.
- [3] Y. Jeong, J. Yoon, *Inorg. Chim. Acta* 381 (2012) 2.
- [4] S.K. Sahoo, D. Sharma, R.K. Bera, G. Crisponi, J.F. Callan, *Chem. Soc. Rev.* 41 (2012) 7195.
- [5] H.N. Kim, W.X. Ren, J.S. Kim, J. Yoon, *Chem. Soc. Rev.* 41 (2012) 3210.
- [6] W.S. Han, H.Y. Lee, S.H. Jung, S.J. Lee, J.H. Jung, *Chem. Soc. Rev.* 38 (2009) 1904.
- [7] C.T. Kresge, M.E. Leonowicz, W.J. Roth, J.C. Vartuli, J.S. Beck, *Nature* 359 (1992) 710.
- [8] R. Métivier, I. Leray, B. Lebeau, B. Valeur, *J. Mater. Chem.* 15 (2005) 2965.
- [9] H.J. Kim, S.J. Lee, S.Y. Park, J.H. Jung, J.S. Kim, *Adv. Mater.* 20 (2008) 3229.
- [10] Z. Jiannan, X. Chuan, F. Qiang, L. Ming, W. Baojun,

- F. Guodong, Y. Hongmei, H. Yanfu, S. Zhiguang, *Nanotechnology* 21 (2010) 045501.
- [11] D. Lu, L. Yang, Z. Tian, L. Wang, J. Zhang, *RSC Adv.* 2 (2012) 2783.
- [12] M. Ganjali, M. Asgari, F. Faridbod, P. Norouzi, A. Badiei, J. Gholami, *J. Solid State Electrochem.* 14 (2010) 1359.
- [13] M. Karimi, A. Badiei, N. Lashgari, J. Afshani, G. Mohammadi Ziarani, *J. Lumin.* 168 (2015) 1.
- [14] M. Hosseini, M.R. Ganjali, Z. Rafiei-Sarmazdeh, F. Faridbod, H. Goldooz, A. Badiei, P. Nourozi, G. Mohammadi Ziarani, *Anal. Chim. Acta* 771 (2013) 95.
- [15] D. Zhao, J. Feng, Q. Huo, N. Melosh, G.H. Fredrickson, B.F. Chmelka, G.D. Stucky, *Science* 279 (1998) 548.
- [16] G. Mohammadi Ziarani, N. Lashgari, A. Badiei, *J. Mol. Catal. A: Chem.* 397 (2015) 166.
- [17] A. Shahbazi, H. Younesi, A. Badiei, *Chem. Eng. J.* 168 (2011) 505.
- [18] L. Hajiaghababaei, B. Ghasemi, A. Badiei, H. Goldooz, M.R. Ganjali, G. Mohammadi Ziarani, *J. Environ. Sci.* 24 (2012) 1347.
- [19] Z. Bahrami, A. Badiei, F. Atyabi, *Chem. Eng. Res. Des.* 92 (2014) 1296.
- [20] Z. Bahrami, A. Badiei, G. Mohammadi Ziarani, *J. Nanopart. Res.* 17 (2015) 125.
- [21] Z. Bahrami, A. Badiei, F. Atyabi, H.R. Darabi, B. Mehravi, *Mater. Sci. Eng. C* 49 (2015) 66.
- [22] L. Gao, Y. Wang, J. Wang, L. Huang, L. Shi, X. Fan, Z. Zou, T. Yu, M. Zhu, Z. Li, *Inorg. Chem.* 45 (2006) 6844.
- [23] M.H. Lim, C.F. Blanford, A. Stein, *Chem. Mater.* 10 (1998) 467.
- [24] A.P. Wight, M.E. Davis, *Chem. Rev.* 102 (2002) 3589.
- [25] M.R. Ganjali, M. Hosseini, Z. Memari, F. Faridbod, P. Norouzi, H. Goldooz, A. Badiei, *Anal. Chim. Acta* 708 (2011) 107.
- [26] M.R. Ganjali, M. Hosseini, F. Aboufazeli, F. Faridbod, H. Goldooz, A.R. Badiei, *Luminescence* 27 (2012) 20.
- [27] M. Hosseini, M. Ganjali, M. Tavakoli, P. Norouzi, F. Faridbod, H. Goldooz, A. Badiei, *J. Fluoresc.* 21 (2011) 1509.
- [28] A. Badiei, H. Goldooz, G. Mohammadi Ziarani, *Appl. Surf. Sci.* 257 (2011) 4912.
- [29] A. Badiei, H. Goldooz, G. Mohammadi Ziarani, A. Abbasi, *J. Colloid Interface Sci.* 357 (2011) 63.
- [30] M. Hosseini, V.K. Gupta, M.R. Ganjali, Z. Rafiei-Sarmazdeh, F. Faridbod, H. Goldooz, A.R. Badiei, P. Norouzi, *Anal. Chim. Acta* 715 (2012) 80.
- [31] M.R. Ganjali, V.K. Gupta, M. Hosseini, Z. Rafiei-Sarmazdeh, F. Faridbod, H. Goldooz, A.R. Badiei, P. Norouzi, *Talanta* 88 (2012) 684.
- [32] F. Faridbod, M.R. Ganjali, M. Hosseini, P. Norouzi, *Int. J. Electrochem. Sci.* 7 (2012) 1927.
- [33] M.R. Ganjali, Z. Rafiei-Sarmazdeh, T. Poursaberi, S.J. Shahtaheri, P. Norouzi, *Int. J. Electrochem. Sci.* 7 (2012) 1908.
- [34] M. Hosseini, M.R. Ganjali, F. Aboufazeli, F. Faridbod, H. Goldooz, A. Badiei, P. Norouzi, *Sensors Actuat. B: Chem.* 184 (2013) 93.
- [35] M. Karimi, A. Badiei, G. Mohammadi Ziarani, *RSC Adv.* 5 (2015) 36530.
- [36] M. Yadavi, A. Badiei, G. Mohammadi Ziarani, *Appl. Surf. Sci.* 279 (2013) 121.
- [37] M. Yadavi, A. Badiei, G. Mohammadi Ziarani, A. Abbasi, *Chem. Pap.* 67 (2013) 751.
- [38] M. Yadavi, A. Badiei, *J. Fluoresc.* 24 (2014) 523.
- [39] P. Zarabadi-Poor, A. Badiei, A.A. Yousefi, J. Barroso-Flores, *J. Phys. Chem. C* 117 (2013) 9281.
- [40] M. Karimi, A. Badiei, G. Mohammadi Ziarani, *J. Fluoresc.* 25 (2015) 1297.